Stem Cell Reports
Article

ISSCR

OPEN ACCESS

Viral delivery of L1CAM promotes axonal extensions by embryonic cerebral grafts in mouse brain

Ryosuke Tsuchimochi,[1,2] Keitaro Yamagami,[1,2] Naoko Kubo,[1] Naoya Amimoto,[1] Fabian Raudzus,[1] Bumpei Samata,[1] Tetsuhiro Kikuchi,[1] Daisuke Doi,[1] Koji Yoshimoto,[2] Aya Mihara,[1] and Jun Takahashi[1,3,*]

[1]Department of Clinical Application, Center for iPS Cell Research and Application, Kyoto University, Kyoto 606-8507, Japan
[2]Department of Neurosurgery, Graduate School of Medical Sciences, Kyushu University, Fukuoka 812-8582, Japan
[3]Department of Neurosurgery, Kyoto University Graduate School of Medicine, Kyoto 606-8507, Japan
*Correspondence: jbtaka@cira.kyoto-u.ac.jp
https://doi.org/10.1016/j.stemcr.2023.02.012

SUMMARY

Cell replacement therapy is expected as a new and more radical treatment against brain damage. We previously reported that transplanted human cerebral organoids extend their axons along the corticospinal tract in rodent brains. The axons reached the spinal cord but were still sparse. Therefore, this study optimized the host brain environment by the adeno-associated virus (AAV)-mediated expression of axon guidance proteins in mouse brain. Among netrin-1, SEMA3, and L1CAM, only L1CAM significantly promoted the axonal extension of mouse embryonic brain tissue-derived grafts. L1CAM was also expressed by donor neurons, and this promotion was exerted in a haptotactic manner by their homophilic binding. Primary cortical neurons cocultured on L1CAM-expressing HEK-293 cells supported this mechanism. These results suggest that optimizing the host environment by the AAV-mediated expression of axon guidance molecules enhances the effect of cell replacement therapy.

INTRODUCTION

The corticospinal tract (CST) is the descending neuronal pathway that originates from the motor cortex and plays an essential role in motor function. Stroke or brain injury often damages the CST and causes motor dysfunction. Medical and surgical treatments followed by rehabilitation improve motor dysfunction to some extent, but the reality is that millions of patients suffer from disabilities after stroke.

Cell replacement therapy is expected as an alternative treatment for brain damage (Grade and Götz, 2017). Previous studies reported that the transplantation of mouse embryonic cortical tissue to injured rodent cerebral cortices results in neurite extension from the graft to the host spinal cord (SC) and provides functional recovery (Gaillard et al., 2007; Péron et al., 2017). We previously reported that cerebral organoids derived from human pluripotent stem cells extend their axons along the CST and reach the spinal cord in intact newborn (postnatal day 7 [P7]) and injured adult (6 week) mouse brains (Kitahara et al., 2020). However, these responses are still insufficient for functional reconstruction of the CST, suggesting that the host brain environment needs to be optimized.

During the development of the neural circuit, a number of axon guidance molecules, such as class 3 semaphorins, netrin-1, and L1CAM, support axonal extension (Canty and Murphy, 2008; Leyva-Díaz and López-Bendito, 2013; Lowery and Vactor, 2009; Stoeckli, 2018). Semaphorin-3A (SEMA3A) and semaphorin-3C (SEMA3C) are mainly involved in early axon outgrowth, and netrin-1 promotes axonal extension to the internal capsule (IC). L1CAM functions later, and L1CAM-deficient mice show dysplasia of the pyramidal decussation and following spinal tracts (Canty and Murphy, 2008; Cohen et al., 1998). The modes of action of these axon guidance molecules are classified into two groups. One is chemotaxis by diffusible chemical cues, and the other is haptotaxis by substrate-bound molecules. Class 3 semaphorins and netrin-1 are extracellular diffusible chemical proteins related to chemotaxis (Lowery and Vactor, 2009). The growth cone, which is the tip of the axon in the elongation process, has specific receptors for these chemical factors. For example, DCC and UNC-5 are receptors for netrin-1, and DCC alone attracts the growth cone, whereas the heterodimer of DCC and UNC-5 repulses it (Boyer and Gupton, 2018; Huber et al., 2003). SEMA3A and SEMA3C bind to neuropilin-1 (NRP1) or neuropilin-2 (NRP2) and transmit signals through their co-receptor, plexinA (Bagnard et al., 1998; Huber et al., 2003; Sharma et al., 2012). L1CAM is a transmembrane cell adhesion molecule that mediates haptotaxis via a homophilic binding mechanism. It plays several critical roles in CNS maturation, including neurite outgrowth, adhesion, fasciculation, migration, myelination, and axon guidance (Barry et al., 2010; Burden-Gulley et al., 1997; Hlavin and Lemmon, 1991; Kamiguchi and Lemmon, 1997; Lemmon et al., 1989).

These findings suggest that the expression of these molecules in the host brain promotes axonal extension from grafted cells, but this assumption has never been investigated. To address this issue, we constructed recombinant adeno-associated virus (rAAV) vectors carrying axon

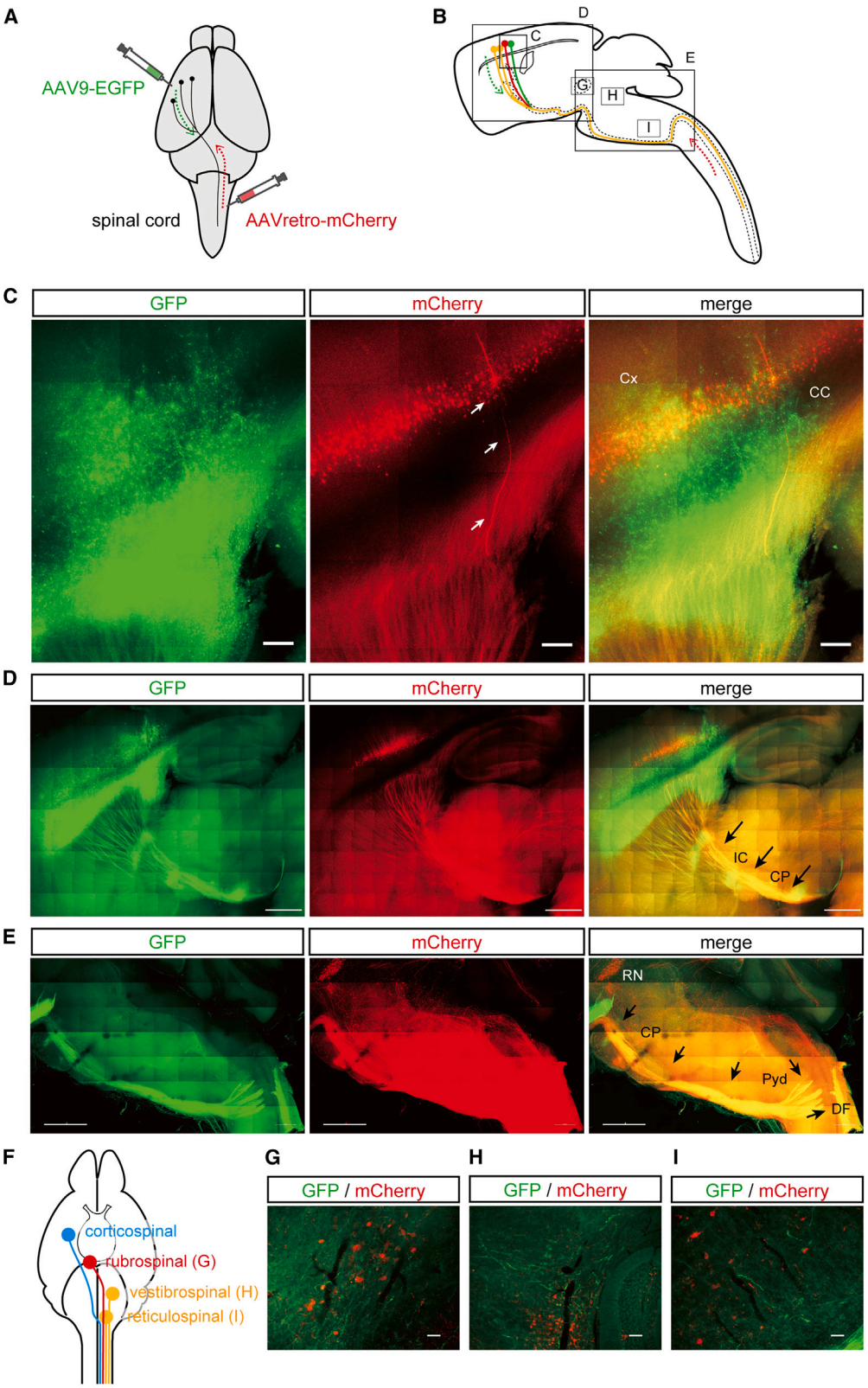

(legend on next page)

guidance molecule genes (Ntn1, Sema3A, Sema3C, and L1cam). First, we injected these rAAV vectors into the host mouse brain and then transplanted embryonic cerebral cortices. We examined axonal extension from the grafts along the CST and found that the number of axons was significantly higher in the L1CAM group than in the control group. These results suggest that the viral delivery of L1CAM into the host brain enhances the therapeutic effects of grafted cortical neurons against brain damage.

RESULTS

Detection of CST by anterograde and retrograde labeling with AAV vector

First, we confirmed that the target protein can be expressed along the CST by injecting rAAV9-EGFP into the motor cortex of adult mice and rAAVretro-mCherry into the intermediate zone of the spinal cord, the terminal of the CST (Wang et al., 2017) (Figures 1A and 1B). Immunofluorescence studies revealed that the CST was labeled by GFP anterogradely and by mCherry retrogradely, resulting in the CST, including pyramidal neurons in the motor cortex, which appeared orange due to the overlap of the green and red signals (Figures 1C–1E and S2). We also detected mCherry+ neuronal cell bodies accompanied by GFP^+ fibers in the red nucleus (RN), vestibular nucleus (VN), and reticular formation (RF), indicating the rubrospinal, vestibulospinal, and reticulospinal pathways, respectively (Lemon, 2008) (Figures 1F–1I).

Viral delivery of L1CAM promoted axonal extension from embryonic cerebral grafts

Regarding the donor tissue, we confirmed that embryonic day 14 (E14.5) mouse cerebral cortex contains subcerebral projecting neurons ($CTIP2^+$) that constitute the CST (Figure 2). L1CAM and DCC were expressed in the cortical plate and intermediate zone, while NRP1 and NRP2 were expressed in these areas and subventricular zone. Double-labeled immunostaining showed that $CTIP2^+$ neurons expressed L1CAM. In addition, $CTIP2^+$ neurons also expressed DCC and NRP, receptors for netrin-1 and class 3 semaphorin, respectively.

We injected rAAV vectors carrying the genes of netrin-1, sema3A, sema3C, L1cam, or mCherry (control) into the motor cortex. One week later, we transplanted the dissected frontal cortex of E14.5 GFP transgenic (Tg) mice (Figure 3A).

Twelve weeks after the cell transplantation, we confirmed that each axon guidance molecule was expressed in the host striatum (Figure 3B). GFP^+ axons derived from the grafts were observed along the host CST including the internal capsule, the cerebral peduncle (CP), and the contralateral spinal cord (Figures 3C and 3D). In addition, we also found GFP^+ axons in the RN, thalamus (Th), the subthalamic nucleus (STh), the substantia nigra (SN), the VN, and the RF. The numbers of GFP^+ axons in the IC, CP, and SC (i.e., along the CST) were significantly higher in the L1CAM group than in the control group (Figure 3E). The numbers were also higher in other areas, such as the RN, STh, SN, VN, and RF, suggesting that L1CAM promoted axonal extension not only along the CST but also into other pathways. Additionally, the number of axons in the SN was significantly higher in the SEMA3A group than in the control group. Still, there was no significant difference in the number of axons in any other region among the other axon guidance molecule groups compared with the control group.

Endogenous and exogenous expression of L1CAM in mouse brain

On the basis of the results above, we focused on L1CAM and investigated the corresponding mechanism. First, we examined the endogenous expression of L1CAM along the CST during development. An immunofluorescence study showed that L1CAM is expressed along the CST until postnatal day 5 (Figure 4A). Its expression became lower after P5 and was rarely seen in adult mice.

Figure 1. Detection of the CST by anterograde and retrograde labeling with the AAV vector

(A) Schematic overview of anterograde and retrograde labeling experiments of the CST in adult mice using AAV vectors.

(B) Schematic of a sagittal section of a mouse brain. Green indicates anterograde labeling, red indicates retrograde labeling, and orange indicates both anterograde and retrograde labeling.

(C–E) 1mm-thick brain sections with tissue clearing. (C) Neurons are labeled by GFP in the anterograde direction from the cortex (Cx) through the corpus callosum (CC). Retrogradely, neurons in layer 5 of the cortex are labeled by mCherry, and Betz cells can be observed extending their axons downward from the cortex through the corpus callosum (arrows). Scale bars, 200 μm. (D) The internal capsule (IC) and the cerebral peduncle (CP) are labeled in the anterograde and retrograde directions. Scale bars, 1,000 μm. (E) Both anterograde and retrograde labeling were observed from the CP to the pyramidal decussation (Pyd) and then to the dorsal funiculus (DF) of the spinal cord. Scale bars, 1,000 μm.

(F) Schematic showing the corticospinal tract, rubrospinal tract, vestibulospinal tract, and reticulospinal tract.

(G–I) The red nucleus (RN) was labeled by mCherry retrogradely. Fibers progressively labeled by GFP were observed in the RN. The same applies to (H) the vestibular nucleus and (I) the reticular formation. Scale bars, 20 μm.

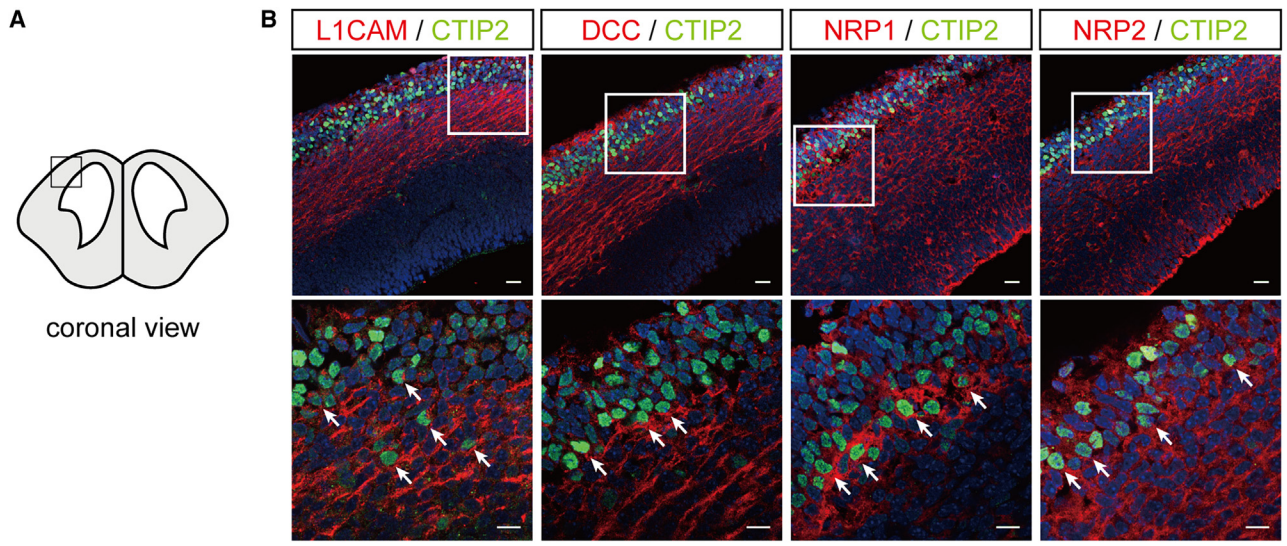

Figure 2. Mouse embryonic cerebral cortex contains subcerebral projecting neurons and proteins that respond to each axon guidance molecule

(A) Schematic of the brain slices of the E14.5 mouse frontal cortex.

(B) Immunofluorescence images for CTIP2 (green), L1CAM (red), DCC (red), NRP1 (red), NRP2 (red), and DAPI (blue). Lower panels are magnified images. Arrows indicate dual positive cells for CTIP2 and L1CAM, DCC, NRP1, and NRP2, respectively. Scale bars, 20 μm (upper) and 10 μm (lower).

Next, to examine the time course of the AAV-mediated expression of L1CAM, we injected rAAV-L1cam/FLAG into the motor cortex of adult mice, and the brains were immunostained by antibodies against L1CAM and FLAG at 1, 3, 7, and 14 days after the injection. The overlapped expression of L1CAM and FLAG was observed in the striatum, the IC, CP, RN, and RF on day 7, and it became higher on day 14 (Figures 4B and S3).

These observations suggested that the axonal extensions might be further promoted if L1CAM was delivered two weeks before the cortical tissue transplantation. Therefore, we injected rAAV-L1cam/FLAG into the mouse frontal cortex and transplanted the cells two weeks later. Again, the numbers of axons along the CST and in the RN and RF were higher in the L1CAM group than in the control group (Figure S4). However, there was no significant difference in the number of axons in each region if the transplants were made one or two weeks after the vector injection (Figure S5).

Graft-derived axons extended along virally expressed L1CAM

L1CAM mediates axonal outgrowth in a haptotactic manner via homophilic binding (Barry et al., 2010; Lemmon et al., 1989). An immunofluorescence study twelve weeks after the transplantation revealed that graft-derived GFP$^+$ axons overlapped with L1CAM and FLAG in the ipsilateral internal capsule (Figure 5A). In an electron microscopic analysis, FLAG-associated L1CAM was observed inside and outside the host axon as well as on their myelin sheath (Figures 5C–5F), and graft-derived GFP$^+$ axons were in contact with host axons expressing L1CAM (Figures 5B and 5F). In addition, we observed two L1CAM stainings very close to each other (Figure 5G). These results indicate that the grafted cells extended axons along virally expressed L1CAM on the host neurons by a haptotactic manner via homophilic binding. We also found synaptic connections between GFP$^+$ axons and host neurons (Figure 5H) and the myelination of GFP$^+$ axons (Figure 5I), suggesting maturation of the graft-derived axons.

To further determine the specificity of the L1CAM effect, we examined the axonal extension in the lateral septum, which receives neuronal connections from the hippocampus, not the motor cortex (Figures S6A–S6C). The AAV-mediated L1CAM/FLAG expression was found in the lateral septum, and the number of GFP$^+$ axons was significantly increased (Figure S6D). Even in such a non-CST site, L1CAM expression promoted axonal extension, indicating that the guidance effect of L1CAM is not pathway specific.

To confirm axonal extensions from the graft to the spinal cord, we injected a retrograde axonal tracer, fast blue (FB), into the cervical spinal cord. We observed FB$^+$ pyramidal neurons in the host motor cortex and GFP$^+$/CTIP2$^+$/FB$^+$ cells in the graft, indicating that the grafted cells extended their axons to the spinal cord (Figure 6).

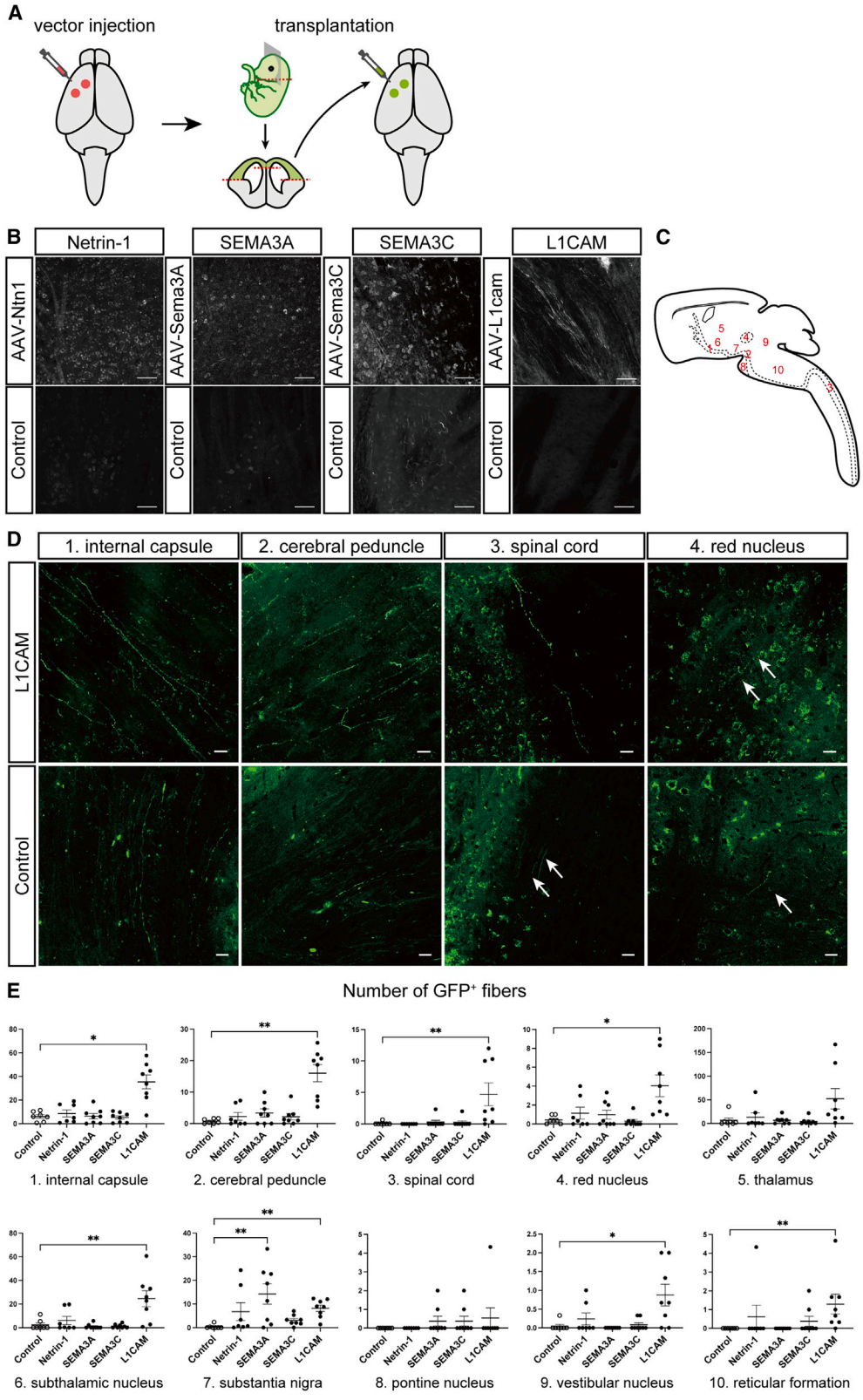

(legend on next page)

L1CAM is also known to be involved in cancer progression and migration (Altevogt et al., 2020). Therefore, we performed double-labeled immunostaining of the grafts for GFP (grated cells) and KI67 (proliferating cells). In both L1CAM and control groups, only a very few cells were KI67 positive, and no double-positive cells (Figure S7). In addition, there were no migrating GFP^+ cells. These results suggest that AAV-mediated L1CAM expression did not affect the proliferative and migratory potential of transplanted cells in this experiment.

$L1CAM^+$ feeder cells promoted neurite extensions by L1CAM-expressing neurons *in vitro*

To investigate the homophilic binding of L1CAM *in vitro*, we produced HEK-293 cells expressing L1CAM by gene transfection using a PiggyBac vector (HEK-L1). The L1CAM expression in these cells was regulated by a Tet-On system. A western blot analysis revealed that HEK-L1 cells expressed L1CAM when treated with doxycycline (DOX). In contrast, wild-type HEK cells and HEK-L1 cells without DOX did not express L1CAM (Figure 7A). We cultured these HEK cells until confluency and plated primary cortical neurons onto the HEK cells. These neurons were derived from the cortical tissue of E14.5 GFP-Tg mouse brains and expressed L1CAM (Figures 7B and 7C). The culture conditions were a combination of with or without DOX and with or without 5G3, an inhibitor of the homophilic binding of L1CAM (Balaian et al., 2000; Wolterink et al., 2010). We measured the neurite length of each cell and compared the average length between the groups (4 independent experiments) for 60 h. After 48 h of observation, the neurite length was significantly longer in the DOX group than control (−/−) group. In addition, 5G3 treatment significantly reduced the neurite length irrespective of the presence of DOX (Figures 7D and 7E). These results support the idea that L1CAM expression by feeder cells promotes the neurite extension of L1CAM-expressing neurons.

DISCUSSION

This study first compared the effect of virally expressed netrin-1, SEMA3, and L1CAM on axonal extension from grafted embryonic cerebral cortices in mouse brain. Only L1CAM significantly promoted axonal extension toward the SC and other areas, including the RN and RF, and these axons were in contact with the expressed L1CAM. *In vitro* observations of primary cortical neurons cocultured on L1CAM-expressing HEK-293 cells supported these findings. These results suggest that the viral expression of L1CAM promotes axonal extension from grafted neurons by a homophilic binding mechanism.

It is known that netrin-1 and SEMA3C attract axons, whereas SEMA3A repels them *in vitro* (Bagnard et al., 1998; Metin et al., 1997). However, in the present study, these chemotactic molecules did not change the neurite extensions of the grafts. Chemorepellent SEMA3A is distributed mainly in the ventricular zone during the developmental stage, while chemoattractant SEMA3C is in the subventricular zone (Bagnard et al., 1998). In addition to these coordinated expressions, diffusible netrin-1 from the ganglion eminence provides the chemoattractant gradient (Metin et al., 1997). Because axonal guidance by diffusible chemical factors is complicated (Canty and Murphy, 2008), our current method might be too simple to expect a significant change. However, appropriate combinations of these molecules, including L1CAM, may further promote axonal extensions from the grafts.

L1CAM is a transmembrane glycoprotein composed of an extracellular domain consisting of six immunoglobulin-like domains and five fibronectin type III-like domains, a single transmembrane domain, and an intracellular domain (Colombo and Meldolesi, 2015; Hortsch, 2000; Maten et al., 2019). It plays several critical roles in CNS maturation, including neurite outgrowth, adhesion, fasciculation, migration, myelination, and axon guidance (Barry et al., 2010; Burden-Gulley et al., 1997; Hlavin and Lemmon, 1991; Kamiguchi and Lemmon, 1997; Lemmon

Figure 3. Viral delivery of L1CAM promoted axonal extension from embryonic cerebral grafts

(A) Schematic of the procedure for the vector injection and transplantation of cortical tissue from E14.5 EGFP Tg mice into the brains of adult mice.

(B) Immunofluorescence images for netrin-1, SEMA3A, SEMA3C, L1CAM in the host striatum 13 weeks after the vector injection. Scale bars, 50 μm.

(C) Schematic showing the CST (dotted area) including the locations of the (1) internal capsule, (2) cerebral peduncle, (3) spinal cord, and (4) red nucleus.

(D) Representative images of GFP^+ neurites at the internal capsule, the cerebral peduncle, the spinal cord, and the red nucleus of the host. Scale bars, 20 μm.

(E) Number of GFP^+ fibers in the (1) internal capsule, (2) cerebral peduncle, (3) spinal cord, (4) red nucleus, (5) thalamus, (6) subthalamic nucleus, (7) substantia nigra, (8) pontine nucleus, (9) vestibular nucleus, and (10) reticular formation of the host. n = 7 for control (mCherry) and netrin-1 groups; n = 8 for SEMA3A, SEMA3C, and L1CAM groups (n, number of mice). $^*p < 0.05$ and $^{**}p < 0.01$, Kruskal-Wallis test with Dunn's multiple-comparisons test. The data are presented as the mean ± SEM.

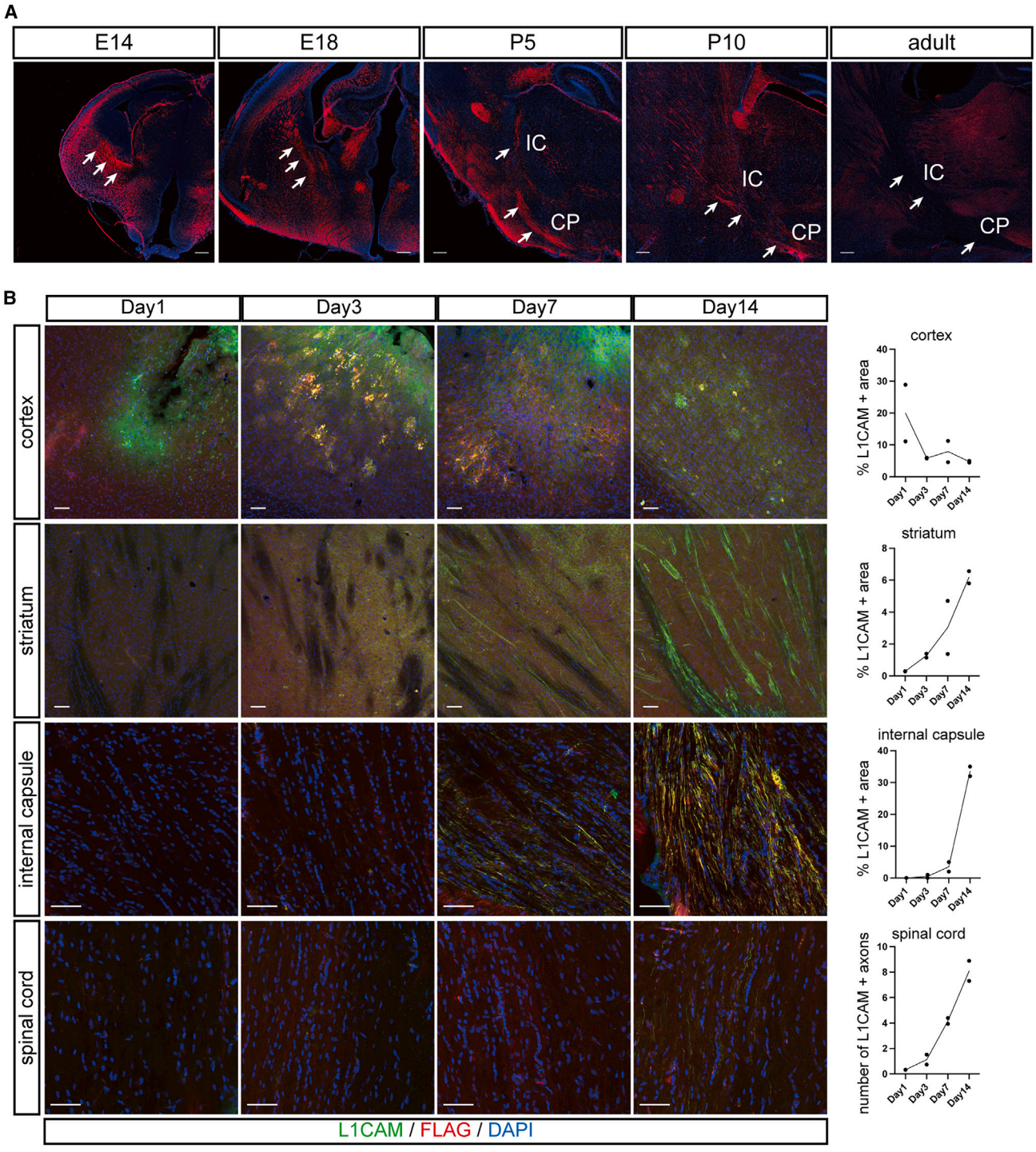

Figure 4. Endogenous and exogenous expression of L1CAM in mouse brain

(A) Natural expression of L1CAM in the CST (arrows) of E14.5, E18.5, P5, P10, and adult mice brains. Scale bars, 100 μm.

(B) Time course expression of L1CAM and FLAG mediated by rAAV injection in the cortex, the striatum, the internal capsule, and the spinal cord. Scale bars, 50 μm. The rightmost column shows the quantitative results for each region: for the cortex, striatum, and internal capsule, the percentage of L1CAM-expressing areas in the image; for the spinal cord, the number of L1CAM-expressing axons.

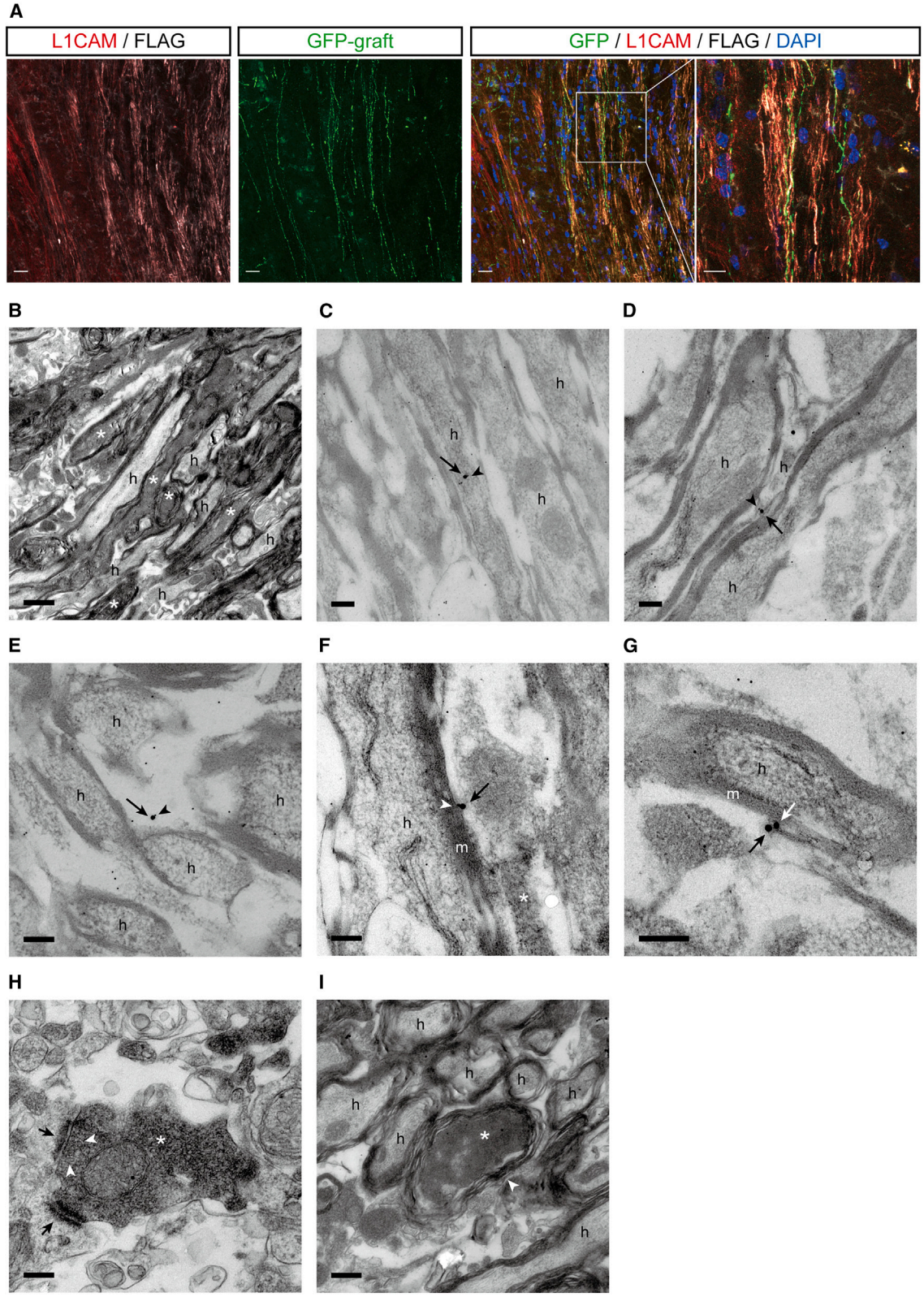

(legend on next page)

et al., 1989). Interestingly, L1CAM was expressed along the CST in the developing brain but not in adults. This observation suggests that L1CAM is necessary for the initial formation of the CST but not for its maintenance. It is possible that the viral delivery of L1CAM in this study reproduced the permissive host environment found in the developing brain to enhance axonal extensions.

Because of the non-specific characteristics of the rAAV vector, L1CAM expression was not restricted to the CST and found in other areas. Accordingly, the number of graft-derived axons increased not only along the CST but also in the RN, VN, and RF. These areas are the origins of the rubrospinal, vestibulospinal, and reticulospinal pathways, respectively. The vestibulospinal and reticulospinal pathways play an essential role in the control of posture maintenance by the trunk muscles and proximal muscles of the upper and lower limbs, while the CST and rubrospinal pathways act on the distal muscle groups and are involved in skilled movements (Lemon, 2008; Lemon et al., 2012). Our results suggest that graft-derived axons can affect these pathways, contributing to motor function.

L1CAM was expressed by both donor neurons and the host brain. Furthermore, graft-derived axons (GFP^+) overlapped with the virally expressed L1CAM in the brain. Electron microscopy showed that the graft-derived axons passed outside the myelin sheath of the host axons, and L1CAM/FLAG expressions were observed outside and on the host myelin sheath. These results suggest that virally expressed L1CAM may be partly distributed on the myelin sheath surface by exocytosis and promotes axonal extensions in a haptotactic manner by homophilic binding (Lemmon et al., 1989).

To confirm this mechanism, we cultured cortical neurons derived from E14.5 mouse brain on L1CAM-expressing HEK-293 cells and found that L1CAM expression enhanced neurite extensions by cortical neurons. The neurite extensions were reduced by an inhibitor of the homophilic binding of L1CAM, 5G3. Intriguingly, this reduction was also found when L1CAM was not expressed by HEK-293 cells. 5G3 inhibits binding to the epitope Ig1 of L1CAM (Balaian et al., 2000; Maten et al., 2019; Wolterink et al., 2010). Additionally, laminin, integrins, contactin, and neurocan are known binding partners of L1CAM involving the Ig1 domain (Grumet, 2003). These results suggested that not only the homophilic binding of L1CAM but also heterophilic binding with these molecules may contribute to the neurite extensions and further explain why the grafted cortical neurons extended axons even in the absence of L1CAM expression.

We have previously reported that mouse embryonic stem cell-derived cortical neurons express L1CAM (Samata et al., 2020). In that study, $L1CAM^+$ cells sorted from the cortical tissue of E14.5 mice contained a higher number of $CTIP2^+$ cells, namely, cerebral projection neurons, and extended longer axons in the mouse brain than L1CAM cells. Thus, the AAV-mediated expression of L1CAM in the host brains of the present study might be helpful to the transplantation of pluripotent stem cell-derived cortical neurons to treat stroke or other neurological diseases.

For gene transfer into organs, several serotypes of AAVs are available, but AAV1, 2, 5, 8, and 9 are commonly used for the CNS (Asokan et al., 2012; Haery et al., 2019; Lisowski et al., 2015; Watakabe et al., 2015). Among these, AAV9 has been reported to have the highest efficiency of gene transfer to cortical neurons in mouse brain when administered directly (Aschauer et al., 2013). As shown in Figure 1, gene expression by AAV9 was found not only along the CST but also in axons toward other areas, such as the RN and RF, resulting in enhanced axonal extensions toward these areas. For more specific gene expression along the CST, we tried retrograde gene expression by injecting AAVretro (Tervo et al., 2016) vector into the spinal cord. Although we succeeded in the retrograde expression of mCherry, the size of L1CAM was too large for this system. We

Figure 5. Graft-derived axons extended along virally expressed L1CAM

(A) Immunohistochemistry for GFP (green), L1CAM (red), and FLAG (white) at the ipsilateral internal capsule. The right column is a magnification of the white square. Scale bars, 20 μm.

(B) Electron micrograph showing that graft-derived axons stained with DAB-labeled GFP (asterisk) extend between host axons (h). Scale bar, 1 μm.

(C-E) L1CAM was detected by the immunogold reaction 25 nm (arrow) and by FLAG 10 nm (arrowhead) inside (C), on the surface (D), and outside (E) of the host axon (h). Scale bars, 200 nm.

(F) L1CAM (arrow) expression accompanied by FLAG (arrowhead) was also found on the myelin sheath (m) of the host axon (h). DAB-labeled GFP^+ axon (asterisk) ran along the L1CAM-expressing host axon. Scale bar, 200 nm.

(G) Homophilic binding between an L1CAM molecule (white arrow) expressed on the myelin sheath (m) of the host axon (h) and another L1CAM molecule (black arrow) was observed. Scale bar, 200 nm.

(H) Synaptic connections (arrows) between a DAB-labeled GFP^+ axon (asterisk) and host neurons. White arrowheads show synaptic vesicles. Scale bar, 200 nm.

(I) Electron micrograph showing that a DAB-labeled GFP^+ axon (asterisk) and host axons (h) were myelinated (arrowhead). Scale bar, 500 nm.

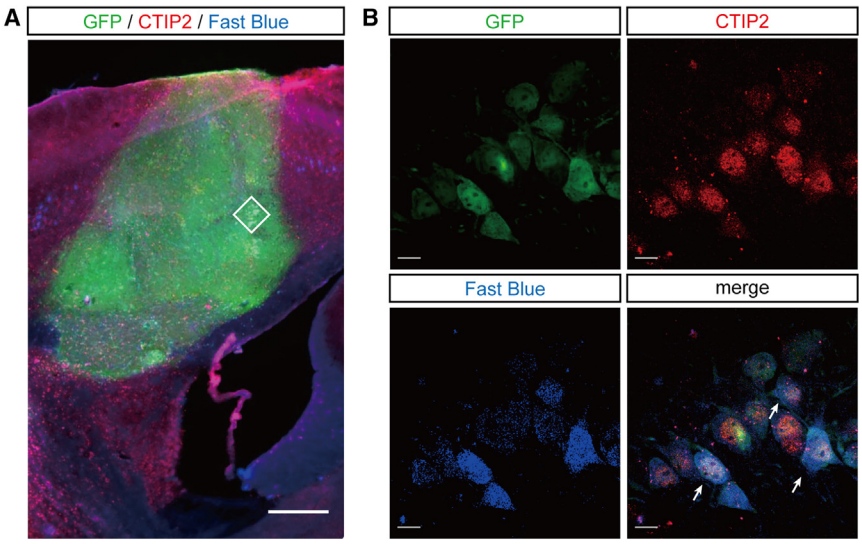

Figure 6. Graft-derived axons extended along the host CST and reach the spinal cord

(A) Low magnification immunohistochemistry image for GFP (green), CTIP2 (red) and fast blue (blue). Scale bar, 300 μm.

(B) High magnification image of the white square in (A). Scale bars, 10 μm.

designed the rAAV vector to include the cytomegalovirus (CMV) promoter because of this promoter's strength at promoting the expression and its compact size (589 bp). A previous study reported that human synapsin has specific transgene expression for corticospinal neurons in mice and rats (Nieuwenhuis et al., 2021). Other combinations of serotype and promoters may improve the specificity of the gene expression.

In this experiment, mouse embryonic cortical tissues were transplanted into normal brains instead of damaged brains. This is because this study aims to examine the effect of the virally expressed axon guidance molecules on transplanted cells. We wanted to minimize uncertainties in the donor cells and the host environment. In CNS injury, however, several axon guidance molecules such as class 3 semaphorins and netrin are upregulated in the acute phase and are thought to play a role in glial scar formation and repelling axon outgrowth to the injured area (Domínguez-Romero and Slater, 2021; Mecollari et al., 2014; Pasterkamp and Verhaagen, 2006). In contrast, L1CAM expression declines from 2 to 16 days after cortical lesion and is expressed in unmyelinated axons and presynaptic terminals two months later, suggesting that it is associated with the maturation of neural connections by reinnervating axon fibers (Schäfer and Frotscher, 2012). Moreover, in CNS injury, myelin-associated proteins, microglia, immune cells, and astrocytes that form glial scars accumulate at the injury site, inhibiting the axonal extension and preventing the repair of the neural circuit (Burda and Sofroniew, 2014; Domínguez-Romero and Slater, 2021; Giger et al., 2010). Therefore, as a next step, it needs to be investigated whether the delivery of axon guidance molecules to the damaged host brain enhances the axonal extension from the grafts after brain injury.

In conclusion, our study showed that the AAV-mediated delivery of L1CAM into mouse brain enhances neurite extensions by the grafted cortical neurons. These results support the idea that optimizing the host environment improves the function of the grafted cells. Such a combination of cell transplantation and gene therapy will enhance the efficiency of treatments for neurological diseases.

EXPERIMENTAL PROCEDURES

Resource availability

Corresponding author

Further information and requests for resources and reagents should be directed to and will be fulfilled by the corresponding author, Jun Takahashi (jbtaka@cira.kyoto-u.ac.jp).

Materials availability

This study did not generate new unique reagents.

Data and code availability

Raw data and images are available upon request to the corresponding author.

Animals

All animal experiments in this study were approved by the Institutional Animal Care and Use Committee of the Animal Research Facility at Kyoto University and conducted according to the Regulations on Animal Experimentation at Kyoto University. All attempts were made to minimize the suffering and the number of animals used in this study. Four thirteen-week-old male mice (C57BL/6NCrSlc) were used for the CST labeling study, 56 thirteen-week-old male mice (C57BL/6NCrSlc) were used as transplanted recipients, and 56 mouse fetuses born from 7 C57BL/6-Tg (CAG-EGFP) mice were used to acquire graft tissues. All mice were purchased from Shimizu Laboratory Supplies Company Limited (Kyoto, Japan). Mice were group-housed under a 12 h light-and-dark cycle, with *ad libitum* access to food and water.

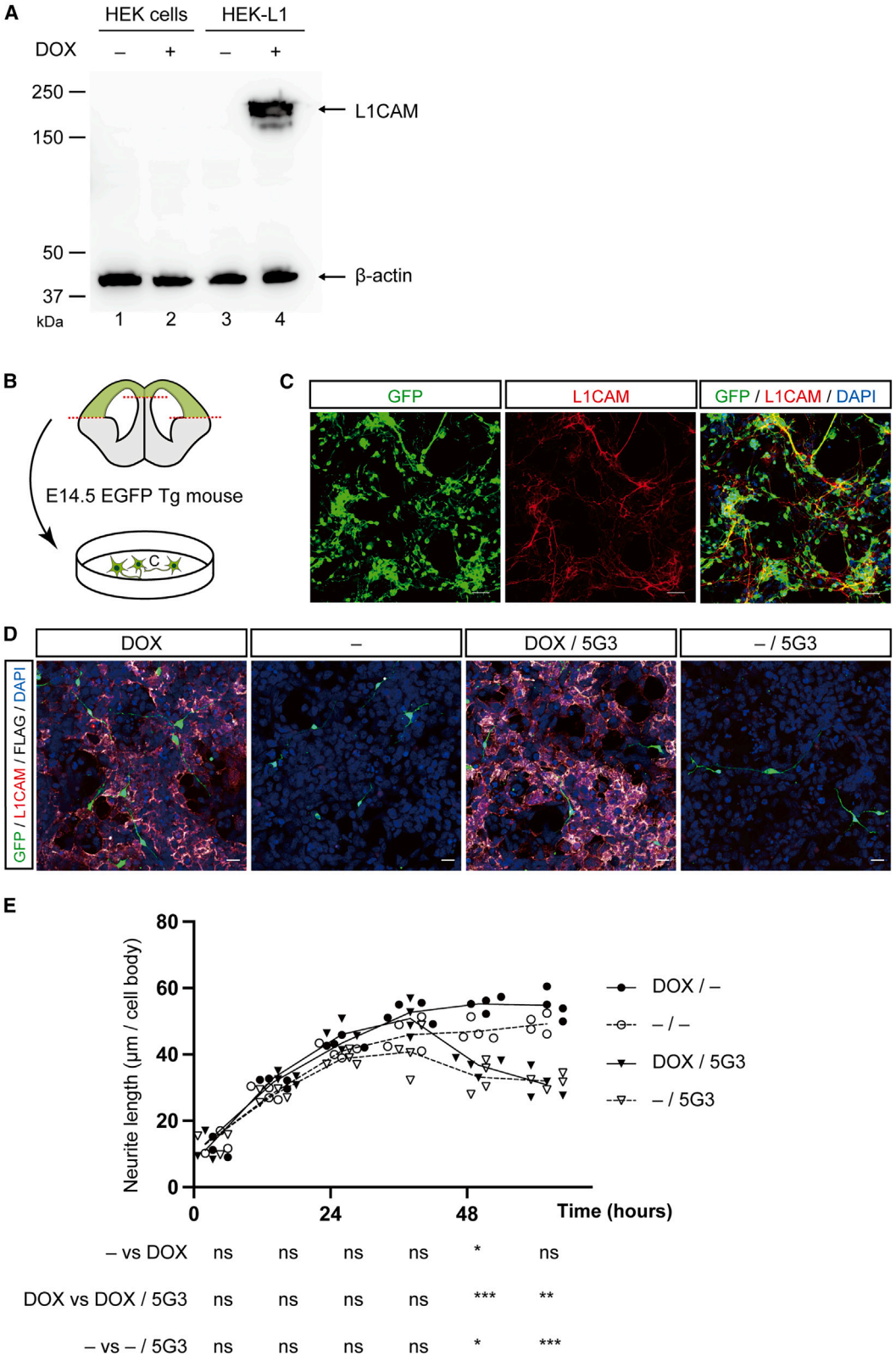

(legend on next page)

Vector

The adeno-associated virus (AAV) vectors used to overexpress axon guidance molecules, pAAV[Exp]-CMV>mL1cam[NM_008478.3]/FLAG (vector ID: VB190707-1042dgs), pAAV[Exp]-CMV>mNtn1[NM_008744.2](ns):T2A:mCherry:WPRE (vector ID: VB190108-1270grn), pAAV[Exp]-CMV>mSema3a[NM_001243072.1](ns):T2A:mCherry:WPRE (vector ID: VB190108-1271fpe), pAAV[Exp]-CMV>mSema3c[NM_013657.5](ns):T2A:mCherry:WPRE (vector ID: VB190108-1273msn), pAAV[Exp]-CMV>EGFP (vector ID: VB150925-10026), and pAAV[Exp]-CMV>mCherry:WPRE (vector ID: VB190114-1227see), were constructed and packaged into AAV9 and AAVretro by VectorBuilder (rAAV9-L1cam/FLAG, rAAV9-Ntn1-mCherry, rAAV9-Sema3A-mCherry, rAAV9-Sema3C-mCherry, rAAV9-EGFP, rAAV9-mCherry, and rAAVretro-mCherry). The vector ID can be used to retrieve detailed information about the vector on vectorbuilder.com. See Figure S1.

Vector injection

Mice were anesthetized with an intraperitoneal injection of a mixture of medetomidine hydrochloride (0.75 mg/kg), midazolam (4 mg/kg), and butorphanol (5 mg/kg) and mounted on a stereotactic apparatus to keep their heads at the horizontal position. A midline scalp incision was performed, and two small windows of the skull over the rostral forelimb area (RFA) of the motor cortex (anterior 1.0 mm, lateral 1.0 mm from the bregma) and the caudal forelimb area (CFA) of the motor cortex (posterior 0.5 mm, lateral 1.8 mm from the bregma) (Wang et al., 2017) were perforated using a drill (Minitor, Tokyo, Japan). Then, 0.3 μL rAAV vector solution (1.0×10^{13} copies/mL) or vehicle (PBS) was injected into the RFA and CFA at depths of 1.0 and 0.5 mm, respectively with a sterile 33G microsyringe (Ito, Shizuoka, Japan).

Cortical tissue harvesting and transplantation

Transplantation was performed on the same day or one week or two weeks after the vector or vehicle injection. The cortical forebrain tissues of E14.5 EGFP transgenic mouse brains were harvested and transferred to Hank's balanced salt solution (HBSS) (Gibco, Gaithersburg, MD) and kept on ice until the transplantation. The tissues were sucked up and transplanted into the RFA and the CFA (as explained above) at depths of 1.0 and 0.5 mm (0.3 μL/site) through a sterile 22G needle (Hamilton, Reno, NV).

Immunostaining

We performed *in vivo* analyses 12 weeks after cell transplantation in all cases. Cell transplantation was performed one week after vector injection, except for one experiment for Figures S4 and S5 with a two-week interval. Twelve weeks after the transplantation, mice were deeply anesthetized with pentobarbital (50 mg/kg, intraperitoneal injection) and transcardially perfused with 4% paraformaldehyde (PFA) (Fujifilm Wako Pure Chemicals, Osaka, Japan). The brains and spinal cords were post-fixed with PFA overnight, transferred to 30% sucrose in PBS, and preserved at 4°C. They were then embedded with O.C.T. compound (Sakura Finetec Japan, Tokyo, Japan) and cut with a cryostat (CM-3050; Leica Biosystems, Buffalo Grove, IL) at 35-μm thickness. The brain sections were preserved in antifreeze (30% glycerol [Nacalai Tesque, Kyoto, Japan], 30% ethylene glycol [Fujifilm Wako Pure Chemicals], and 40% PBS) at −30°C until use. The sections were permeabilized with 0.3% Triton X-100 (Sigma-Aldrich, St. Louis, MO) in PBS (room temperature, 45 min) and blocked in 2% skim milk (BD Biosciences, San Jose, CA) in PBS (room temperature, 30 min) and incubated with primary antibodies (4°C, overnight) followed by incubation with secondary antibodies conjugated with Alexa 488, 594, and 647 (room temperature, 2 h). Nuclear staining was performed with 4′,6-diamidino-2-phenylindole (DAPI). The primary antibodies used were rat anti-L1CAM antibody (1:500; #MAB5674; R&D Systems, Minneapolis, MN), mouse anti-L1CAM antibody (1:500; #ab24345; Abcam, Cambridge, UK), rabbit anti-NRP1 antibody (1:500; #AB10521; EMD Millipore Corporation, Temecula, CA), rabbit anti-NRP2 antibody (1:500; #AB10522; EMD Millipore Corporation), goat anti-DCC antibody (1:1,000; #sc-6535; Santa Cruz Biotechnology, Heidelberg Germany), rat anti-CTIP2 antibody (1:1,000; #ab18465; Abcam), rabbit anti-GFP antibody (1:1,000; #598; Medical and Biological Laboratories, Nagoya, Japan), mouse anti-FLAG M2 antibody (1:1,000; #F1804; Sigma-Aldrich), rabbit anti-KI67 antibody (1:500; #ab16667; Abcam), and rabbit anti-mCherry antibody (1:500; #ab167453; Abcam). Images were visualized using a confocal laser microscope (LSM700 [Carl Zeiss, Thornwood, NY], CQ1 [Yokogawa Electric, Ishikawa, Japan]) and BZ-X710 (Keyence, Osaka, Japan). Maximum intensity projection (MIP) images of GFP/DAPI were made using CellPathfinder software (Yokogawa Electric) and converted to tiled figures using Fiji software (Schindelin et al., 2012). Nine sections in each mouse were used for the analysis. The number of axons derived from a graft labeled by the anti-GFP antibody was manually counted in the three sagittal sections for each region. All the fibers were measured, and the numbers of the fibers were averaged for each animal. Quantification of L1CAM expression was also analyzed using Fiji software. The L1CAM signal was binarized, and the percentage of signal-positive areas in the

Figure 7. L1CAM$^+$ cells promoted neurite outgrowth by homophilic binding *in vitro*

(A) Western blotting for L1CAM, FLAG, and β-actin (a loading control) in wild-type HEK-293 cells (HEK cells) and L1CAM/FLAG-expressing HEK-293 cells (HEK-L1). Lane 1: HEK cells without doxycycline (DOX); lane 2: HEK cells with DOX; lane 3: HEK-L1 without DOX; lane 4: HEK-L1 with DOX.

(B and C) Immunohistochemistry for GFP and L1CAM of a cultured primary neuron dissociated at E14.5. Scale bars, 100 μm.

(D) Representative images of GFP$^+$ neurites on HEK-L1 with or without DOX (left two panels) and with 5G3 (right two panels). Scale bars, 20 μm.

(E) Quantitative analysis of time course changes in the neurite length of primary neurons on HEK-L1. The experiment was repeated four times using quadruplicates for each group. *$p < 0.05$, **$p < 0.01$, and ***$p < 0.001$, repeated-measures two-way ANOVA with Tukey's multiple-comparisons test.

image was calculated. The images used for this analysis were taken randomly, four (320 × 320 μm) for each area, and the quantified values were averaged.

Tissue clearing

Anesthetized mice were mounted on a stereotactic apparatus. First, 0.3 μL AAV9-GFP solution (1.0×10^{13} copies/mL) was injected into the left RFA and CFA as explained above. Next, a midline skin incision was made from the level of the posterior auricle to the level of the superior margin of the scapula, followed by an incision of the superficial muscles and blunt dissection of the deeper muscles. A right hemilaminectomy from C3 to C7 was performed and a dura mater incision followed. Then, 0.1 μL rAAVretro-mCherry was injected at a depth of 0.5 mm just medial to the entry zone of the dorsal rootlet at five points from spinal cord segments C3 to C7, targeting the intermediate zone (the terminal of the CST [Lepore, 2011; Wang et al., 2017]).

Three weeks after the vector injection, the mice were sacrificed and perfusion-fixed by 4% PFA. The cerebrospinal cords were removed and post-fixed in 4% PFA overnight at 4°C and were washed in PBS for 2 h three times at room temperature. To visualize the CST in the same plane, the cerebrospinal cords were sectioned in 1 mm angled sagittal thick sections. The tissue clearing procedure was performed as described previously (Susaki et al., 2014, 2015). Briefly, the cerebrospinal cords were incubated in CUBIC-L (#T3740; Tokyo Chemical Industry, Tokyo, Japan) for five days at 37°C. After washing in PBS for 2 h three times at room temperature, the samples were incubated in CUBIC-R+ (#T3741; Tokyo Chemical Industry) for more than 3 days at 37°C.

Images were visualized using a confocal laser microscope (LSM700) and tiled and z stacked with its software.

Retrograde labeling

Fast blue (Polysciences, Warrington, PA) was used for the retrograde labeling studies. To label transplanted cells that extend axons to the spinal cord along the CST, solution containing 4% (v/w) FB, 4% (v/v) dimethyl sulfoxide (Merck), and artificial cerebrospinal fluid (Harvard Apparatus, Holliston, MA) was injected into the pyramidal decussation 7 days before sacrifice.

Electron microscopy

The brain sections were washed twice with PBS and incubated for 15 min with PBS containing 0.3% H_2O_2 and 0.4% Photo-Flo (Kodak, Rochester, NY). After three 10 min washes with PBS, the sections were blocked in 2% skim milk (BD Biosciences) in PBS for 1 h at room temperature and incubated with rabbit anti-GFP antibody (1:1,000; #598) in 2% skim milk in PBS overnight at 4°C. After three 10 min washes with PBS, the sections were incubated with biotin-conjugated goat anti-rabbit IgG antibody in 2% skim milk in PBS for 2 h at room temperature and washed with PBS three times for 10 min. The sections were then reacted with avidin-biotin complex (Vector Laboratories, Burlingame, CA) for 1 h at room temperature. After three 10 min washes with PBS, the sections were reacted with 0.02% 3,3′-diaminobenzidine, tetrahydrochloride (DAB-4HCl; Dojindo, Kumamoto, Japan) and 0.0002% H_2O_2 in 50 mM Tris-HCl (pH 7.6) for 20 min at room temperature. After dehydration, the sections were flat-embedded in epoxy resin and cut into ultra-thin sections at 70 nm thickness with an ultramicrotome (EM UC6; Leica Biosystems). After washing with PBS, the sections were blocked with 5% bovine serum albumin (BSA; Fujifilm Wako Pure Chemicals) for 5 min. The sections were then reacted with primary antibodies (rat anti-L1CAM antibody [1:30; #MAB5674] and mouse anti-FLAG M2 antibody [1:30; #F1804]) at 4°C overnight. The sections were then washed with PBS (7 times, 1 min each) and reacted with secondary antibodies (goat anti-rat IgG [25 nm Gold] [1:30; #ab41513; Abcam] and goat anti-mouse IgG [10 nm Gold] [1:30; #ab39619; Abcam]) at room temperature for 2 h. After washing with PBS, the sections were fixed with 2% Glutaraldehyde (Fujifilm Wako Pure Chemicals) diluted in PBS for 15 min and washed with distilled water (DW). The sections were then stained with uranyl acetate and lead citrate and examined with an electron microscope (JEM1400Flash; JEOL, Tokyo, Japan). Transmission electron microscopy was performed at the Division of Electron Microscopic Study, Center for Anatomical Studies, Graduate School of Medicine, Kyoto University.

Transfection and production of L1CAM-expressing HEK-293 cells

The DNA segment encoding L1CAM/FLAG was PCR amplified from pAAV[Exp]-CMV>mL1cam[NM_008478.3]/FLAG (vector ID: VB190707-1042dgs), followed by digestion with EcoRI and sac II using 15 bp overlap primers as described in the Clontech In-Fusion user manual. PiggyBac transposon plasmid (VB201202-1242kvw) containing tetracycline-responsive element promotor (TRE3G), improved reverse tetracycline-responsive transcriptional activator (TetOn3G), and puromycin resistance gene (Puro) was linearized by PCR with overlap primers, and the L1cam/FLAG PCR product was ligated via In-Fusion (Clontech, Mountain View, CA). HEK-293 cells were maintained in DMEM (Sigma-Aldrich) supplemented with 10% fetal bovine serum (FBS; Merck), 100 U/mL penicillin, and 100 μg/mL streptomycin (Gibco).

HEK-293 cells were detached by Trypsin in PBS and centrifuged for 3 min at 200 × *g*. The supernatant was discarded, and the pellet was resuspended in 1 mL DMEM. After determining the cell number, 1×10^6 HEK-293 cells were transferred into a new 1.5-mL reaction tube and centrifuged again under the conditions described above. The supernatant was discarded, and the pellet was resuspended in 100 μL Opti-MEM I (Gibco). One microgram of PB Tet-On-L1CAM/FLAG plasmid and 1 μg pCAG-Pbase (Kim et al., 2015) (a kind gift of Dr. Knut Woltjen) were added to the cell suspension, which was then transferred to an electroporation cuvette (2 mm gap; Nepa Gene, Chiba, Japan). The electroporation was performed with the P023 program using Nucleofector 2b (Lonza, Basel, Switzerland). After 2 days of incubation, 1 μg/mL of Puromycin was added for the selection.

After 5 days of selection, the cells were passaged.

Western blotting

Wild-type and L1CAM/FLAG-expressing HEK-293 cells were seeded at 300,000 cells/well and cultured in 6-well plates. After they became confluent, the cell culture dishes were placed on ice and the cells were washed with ice-cold PBS. After aspirating the PBS, ice-cold RIPA buffer (150 mM sodium chloride, 1.0% Triton X-100, 0.5% sodium deoxycholate, 0.1% SDS (sodium dodecyl sulfate), 50 mM Tris with pH 8.0, and 1:100 protease inhibitor cocktail

in distilled water) (0.5 mL per well). The cells were then transferred into pre-cooled microcentrifuge tubes and stored at 4°C for 30 min. The tubes were then centrifuged at 4°C for 20 min at 12,000 rpm. The supernatant was collected and the concentration of the protein was measured using the Pierce BCA Protein Assay Kit (Thermo Science; REF 23227) and an absorbance microplate reader. Equal amounts of protein (10 μg) were denatured at 95°C for 5 min in 2× Laemmli Sample Buffer (Bio-Rad, Hercules, CA) with 10% 2-mercaptoethanol. The samples were then loaded to Any kD Mini-PROTEAN TGX Precast Protein Gels (Bio-Rad) wells. Five microliters of Precision Plus Protein WesternC Protein Standards (Bio-Rad) with 1 μL StrepTactin-HRP conjugate (Bio-Rad) was loaded for the marker. Electrophoresis was performed under Running Buffer (10% 10×Tris/Glycine/SDS buffer [Bio-Rad] in DW) at 200 V, 0.06 A, and 300 W for 30 min. The gels were transferred to an Immun-Blot PVDF Membrane (Bio-Rad) by electroblotting in blotting buffer (8% 10×Tris/Glycine [Bio-Rad] and 20% MeOH in DW) at 100 V, 3.00 A, and 300 W for 90 min. The membranes were blocked in 5% skim milk in Tris-buffered saline containing 0.1% Tween 20 (TBST) for 1 h at room temperature and incubated with primary antibodies (rat anti-L1CAM [1:5,000; #MAB5674] and mouse anti-β-actin [1:5,000; #A2228; Sigma-Aldrich]) overnight at 4°C followed by incubation with horseradish peroxidase-conjugated secondary antibody (anti-rat IgG-HRP (1:10,000; #sc-2006; Santa Cruz) and anti-mouse IgG-HRP (1:10,000; #ab6820; Abcam) for 90 min at room temperature. The signal was detected using Pierce ECL Plus Western Blotting Substrate (Thermo Fisher Scientific). Images were acquired using ImageQuant LAS4000 (Cytiva, Tokyo, Japan).

In vitro assay

For the *in vitro* assay, 10,000 HEK-293 cells (PB-L1Cam/FLAG) per well were plated on a collagen (COSMO)-coated 96-well plate and incubated at 37°C. Doxycycline (100 ng/mL; Clontech) was added to the medium to induce Tet-On gene expression and retained throughout the entire experiment. After the cells formed a confluent monolayer, proliferation was stopped by the addition of 100 ng/mL mitomycin and subsequently incubated for 2 h at 37°C to stop proliferation. E14.5 cortical neurons from EGFP transgenic mice were harvested, enzymatically dissociated using Neuron Dissociation Solutions (Fujifilm Wako Pure Chemicals), and suspended in Neuron Culture Medium (Fujifilm Wako Pure Chemicals) supplemented with 10% FBS. The neurons were then seeded at a density of 10,000 cells/cm^2 on the cultured HEK cells described above. As a negative control, 1:200 anti-L1CAM monoclonal antibody (mAb) 5G3 was added to the medium; 5G3 is known to inhibit the homophilic binding of L1CAM (Balaian et al., 2000; Wolterink et al., 2010). The images were obtained every 12 h using IncuCyte S3 (Sartorius, Goettingen, Germany), and the GFP-positive neurite length was automatically measured using IncuCyte Neurotrack software (Sartorius). The experiment was repeated four times in quadruplicate.

Statistical analysis

Statistical analyses were performed using Prism 9 (GraphPad Software). For comparisons in the *in vivo* experiment, the significances of differences were determined using Mann-Whitney test for comparison of two groups and the Kruskal-Wallis test with Dunn's multiple-comparisons test for comparison of three or more groups (both tests are unpaired and nonparametric). For the *in vitro* experiments, the significances of differences were determined by repeated-measures two-way ANOVA with Tukey's multiple-comparisons test. Differences were considered statistically significant when probability values were <0.05. The data are presented as the mean ± SEM.

SUPPLEMENTAL INFORMATION

Supplemental information can be found online at https://doi.org/10.1016/j.stemcr.2023.02.012.

AUTHOR CONTRIBUTIONS

R.T. and J.T. designed the project. R.T., Keitaro Yamagami, N.K., N.A., B.S., T.K., and D.D. performed the experiments. F.R. assisted with the transfection experiments. R.T. analyzed the data. R.T. wrote the original draft. J.T. reviewed and edited the manuscript. Koji Yoshimoto and J.T. supervised the research. J.T. obtained grants for the research. All authors approved the final manuscript as submitted.

ACKNOWLEDGMENTS

We thank Keiko Okamoto-Furuta and Haruyasu Kohda (Division of Electron Microscopic Study, Center for Anatomical Studies, Graduate School of Medicine, Kyoto University) for technical assistance with the electron microscopy; Knut Woltjen for kindly providing pCAG-PBase; Aya Mihara for technical support with the animal experiments; Kei Kubota for taking care of the animals; Peter Karagiannis for critical reading of the manuscript; and all members of the Takahashi lab for discussions. This work was supported by a grant from the Network Program for Realization of Regenerative Medicine from the Japan Agency for Medical Research and Development (AMED) (21bm0104001h0009 and 21bm0204004h0009) (to J.T.).

CONFLICT OF INTERESTS

The authors declare no competing interests.

Received: June 21, 2022
Revised: February 24, 2023
Accepted: February 25, 2023
Published: March 23, 2023

REFERENCES

Altevogt, P., Ben-Ze'ev, A., Gavert, N., Schumacher, U., Schäfer, H., and Sebens, S. (2020). Recent insights into the role of L1CAM in cancer initiation and progression. Int. J. Cancer *147*, 3292–3296.

Aschauer, D.F., Kreuz, S., and Rumpel, S. (2013). Analysis of transduction efficiency, tropism and axonal transport of AAV serotypes 1, 2, 5, 6, 8 and 9 in the mouse brain. PLoS One *8*, e76310.

Asokan, A., Schaffer, D.V., and Samulski, R.J. (2012). The AAV vector toolkit: poised at the clinical crossroads. Mol. Ther. *20*, 699–708.

Bagnard, D., Lohrum, M., Uziel, D., Püschel, A.W., and Bolz, J. (1998). Semaphorins act as attractive and repulsive guidance signals during the development of cortical projections. Development *125*, 5043–5053.

Balaian, L.B., Moehler, T., and Montgomery, A.M. (2000). The human neural cell adhesion molecule L1 functions as a costimulatory molecule in T cell activation. Eur. J. Immunol. *30*, 938–943.

Barry, J., Gu, Y., and Gu, C. (2010). Polarized targeting of L1-CAM regulates axonal and dendritic bundling in vitro. Eur. J. Neurosci. *32*, 1618–1631.

Boyer, N.P., and Gupton, S.L. (2018). Revisiting netrin-1: one who guides (axons). Front. Cell. Neurosci. *12*, 221.

Burda, J.E., and Sofroniew, M.V. (2014). Reactive gliosis and the multicellular response to CNS damage and disease. Neuron *81*, 229–248.

Burden-Gulley, S.M., Pendergast, M., and Lemmon, V. (1997). The role of cell adhesion molecule L1 in axonal extension, growth cone motility, and signal transduction. Cell Tissue Res. *290*, 415–422.

Canty, A.J., and Murphy, M. (2008). Molecular mechanisms of axon guidance in the developing corticospinal tract. Prog. Neurobiol. *85*, 214–235.

Cohen, N.R., Taylor, J.S., Scott, L.B., Guillery, R.W., Soriano, P., and Furley, A.J. (1998). Errors in corticospinal axon guidance in mice lacking the neural cell adhesion molecule L1. Curr. Biol. *8*, 26–33.

Colombo, F., and Meldolesi, J. (2015). L1-CAM and N-CAM: from adhesion proteins to pharmacological targets. Trends Pharmacol. Sci. *36*, 769–781.

Domínguez-Romero, M.E., and Slater, P.G. (2021). Unraveling axon guidance during axotomy and regeneration. Int. J. Mol. Sci. *22*, 8344.

Gaillard, A., Prestoz, L., Dumartin, B., Cantereau, A., Morel, F., Roger, M., and Jaber, M. (2007). Reestablishment of damaged adult motor pathways by grafted embryonic cortical neurons. Nat. Neurosci. *10*, 1294–1299.

Giger, R.J., Hollis, E.R., and Tuszynski, M.H. (2010). Guidance molecules in axon regeneration. Cold Spring Harb. Perspect. Biol. *2*, a001867.

Grade, S., and Götz, M. (2017). Neuronal replacement therapy: previous achievements and challenges ahead. Npj Regen. Med. *2*, 29.

Grumet, M. (2003). The L1CAM extracellular region a multi-domain protein with modular and cooperative binding modes. Front. Biosci. *8*, s1210–s1225.

Haery, L., Deverman, B.E., Matho, K.S., Cetin, A., Woodard, K., Cepko, C., Guerin, K.I., Rego, M.A., Ersing, I., Bachle, S.M., et al. (2019). Adeno-associated virus technologies and methods for targeted neuronal manipulation. Front. Neuroanat. *13*, 93.

Hlavin, M.L., and Lemmon, V. (1991). Molecular structure and functional testing of human L1CAM: an interspecies comparison. Genomics *11*, 416–423.

Hortsch, M. (2000). Structural and functional evolution of the L1 family: are four adhesion molecules better than one? Mol. Cell. Neurosci. *15*, 1–10.

Huber, A.B., Kolodkin, A.L., Ginty, D.D., and Cloutier, J.-F. (2003). Signaling at the growth cone: ligand-receptor complexes and the control of axon growth and guidance. Annu. Rev. Neurosci. *26*, 509–563.

Kamiguchi, H., and Lemmon, V. (1997). Neural cell adhesion molecule L1: signaling pathways and growth cone motility. J. Neurosci. Res. *49*, 1–8.

Kim, S.-I., Oceguera-Yanez, F., Sakurai, C., Nakagawa, M., Yamanaka, S., and Woltjen, K. (2015). Inducible transgene expression in human iPS cells using versatile all-in-one piggyBac transposons. In Methods in Molecular Biology (Humana Presspp), pp. 111–131.

Kitahara, T., Sakaguchi, H., Morizane, A., Kikuchi, T., Miyamoto, S., and Takahashi, J. (2020). Axonal extensions along corticospinal tracts from transplanted human cerebral organoids. Stem Cell Rep. *15*, 467–481.

Lemmon, V., Farr, K.L., and Lagenaur, C. (1989). L1-mediated axon outgrowth occurs via a homophilic binding mechanism. Neuron *2*, 1597–1603.

Lemon, R.N. (2008). Descending pathways in motor control. Annu. Rev. Neurosci. *31*, 195–218.

Lemon, R.N., Landau, W., Tutssel, D., and Lawrence, D.G. (2012). Lawrence and Kuypers (1968a,b) revisited Copies of the original filmed material from their classic papers in Brain. Brain *135*, 2290–2295.

Lepore, A.C. (2011). Intraspinal cell transplantation for targeting cervical ventral horn in amyotrophic lateral sclerosis and traumatic spinal cord injury. J. Vis. Exp. *55*, 3069.

Leyva-Díaz, E., and López-Bendito, G. (2013). In and out from the cortex: development of major forebrain connections. Neuroscience *254*, 26–44.

Lisowski, L., Tay, S.S., and Alexander, I.E. (2015). Adeno-associated virus serotypes for gene therapeutics. Curr. Opin. Pharmacol. *24*, 59–67.

Lowery, L.A., and Van Vactor, D. (2009). The trip of the tip: understanding the growth cone machinery. Nat. Rev. Mol. Cell Biol. *10*, 332–343.

Maten, M.v.d., Reijnen, C., Pijnenborg, J.M.A., and Zegers, M.M. (2019). L1 cell adhesion molecule in cancer, a systematic review on domain-specific functions. Int. J. Mol. Sci. *20*, 4180.

Mecollari, V., Nieuwenhuis, B., and Verhaagen, J. (2014). A perspective on the role of class iii semaphorin signaling in central nervous system trauma. Front. Cell. Neurosci. *8*, 328.

Métin, C., Deléglise, D., Serafini, T., Kennedy, T.E., and Tessier-Lavigne, M. (1997). A role for netrin-1 in the guidance of cortical efferents. Development *124*, 5063–5074.

Nieuwenhuis, B., Haenzi, B., Hilton, S., Carnicer-Lombarte, A., Hobo, B., Verhaagen, J., and Fawcett, J.W. (2021). Optimization of adeno-associated viral vector-mediated transduction of the corticospinal tract: comparison of four promoters. Gene Ther. *28*, 56–74.

Pasterkamp, R.J., and Verhaagen, J. (2006). Semaphorins in axon regeneration: developmental guidance molecules gone wrong? Philos. Trans. R. Soc. Lond. B Biol. Sci. *361*, 1499–1511.

Péron, S., Droguerre, M., Debarbieux, F., Ballout, N., Benoit-Marand, M., Francheteau, M., Brot, S., Rougon, G., Jaber, M., and Gaillard, A. (2017). A delay between motor cortex lesions and neuronal

transplantation enhances graft integration and improves repair and recovery. J. Neurosci. *37*, 1820–1834.

Samata, B., Takaichi, R., Ishii, Y., Fukushima, K., Nakagawa, H., Ono, Y., and Takahashi, J. (2020). L1CAM is a marker for enriching corticospinal motor neurons in the developing brain. Front. Cell. Neurosci. *14*, 31.

Schäfer, M.K.E., and Frotscher, M. (2012). Role of L1CAM for axon sprouting and branching. Cell Tissue Res. *349*, 39–48.

Schindelin, J., Arganda-Carreras, I., Frise, E., Kaynig, V., Longair, M., Pietzsch, T., Preibisch, S., Rueden, C., Saalfeld, S., Schmid, B., et al. (2012). Fiji: an open-source platform for biological-image analysis. Nat. Methods *9*, 676–682.

Sharma, A., Verhaagen, J., and Harvey, A.R. (2012). Receptor complexes for each of the class 3 Semaphorins. Front. Cell. Neurosci. *6*, 1–13.

Stoeckli, E.T. (2018). Understanding axon guidance: are we nearly there yet? Development *145*, dev151415.

Susaki, E.A., Tainaka, K., Perrin, D., Kishino, F., Tawara, T., Watanabe, T.M., Yokoyama, C., Onoe, H., Eguchi, M., Yamaguchi, S., et al. (2014). Whole-brain imaging with single-cell resolution using chemical cocktails and computational analysis. Cell *157*, 726–739.

Susaki, E.A., Tainaka, K., Perrin, D., Yukinaga, H., Kuno, A., and Ueda, H.R. (2015). Advanced CUBIC protocols for whole-brain and whole-body clearing and imaging. Nat. Protoc. *10*, 1709–1727.

Tervo, D.G.R., Hwang, B.-Y., Viswanathan, S., Gaj, T., Lavzin, M., Ritola, K.D., Lindo, S., Michael, S., Kuleshova, E., Ojala, D., et al. (2016). A designer AAV variant permits efficient retrograde access to projection neurons. Neuron *92*, 372–382.

Wang, X., Liu, Y., Li, X., Zhang, Z., Yang, H., Zhang, Y., Williams, P.R., Alwahab, N.S.A., Kapur, K., Yu, B., et al. (2017). Deconstruction of corticospinal circuits for goal-directed motor skills. Cell *171*, 440–455.e14.

Watakabe, A., Ohtsuka, M., Kinoshita, M., Takaji, M., Isa, K., Mizukami, H., Ozawa, K., Isa, T., and Yamamori, T. (2015). Comparative analyses of adeno-associated viral vector serotypes 1, 2, 5, 8 and 9 in marmoset, mouse and macaque cerebral cortex. Neurosci. Res. *93*, 144–157.

Wolterink, S., Moldenhauer, G., Fogel, M., Kiefel, H., Pfeifer, M., Lüttgau, S., Gouveia, R., Costa, J., Endell, J., Moebius, U., et al. (2010). Therapeutic antibodies to human L1CAM: functional characterization and application in a mouse model for ovarian carcinoma. Cancer Res. *70*, 2504–2515.